Desalination and Water Treatment
www.deswater.com

doi: 10.5004/dwt.2020.25869

194 (2020) 214–221
August

Examination of azophloxine degradation on porous lanthanum titanate synthesized via a polyethylene glycol mediated sol–gel route

Meihua Lian, Zheng Ma, Wenjie Zhang*

School of Environmental and Chemical Engineering, Shenyang Ligong University, Shenyang 110159, China, email: wjzhang@aliyun.com (W. Zhang)

Received 7 October 2019; Accepted 20 March 2020

ABSTRACT

Porous lanthanum titanate photocatalyst was synthesized via a sol–gel route by adding polyethylene glycol (PEG2000) in the precursor. Photocatalytic degradation of azophloxine on the porous lanthanum titanate was studied. The azophloxine solution during photocatalytic degradation was analyzed using Fourier transform infrared (FT-IR) spectroscopy, UV-visible (UV-Vis) spectrometry, total organic carbon analysis, and ion chromatography. The degradation of benzene ring, naphthalene ring, C–N bond, and R–SO_3^- in the azophloxine molecule is proven by the reduced absorption intensities in the UV-Vis and FT-IR spectra. The large azophloxine molecule is broken up at the beginning, and the organic substances can be subsequently degraded. Mineralization of the organic substances is slower than decoloration of the dye. The variation of Na^+, NH_4^+, NO_2^-, NO_3^-, and SO_4^{2-} concentrations in the azophloxine solution with prolonged irradiation time can indicate azophloxine mineralization. The final degradation products of nitrogen are NH_4^+ and NO_3^- ions. The total ionic nitrogen concentration in the solution increases with rising reaction time, depending on the activity of the materials.

Keywords: $La_2Ti_2O_7$; Photocatalytic; Azophloxine; Degradation; PEG2000

1. Introduction

Hazardous organic substances have detrimental effects on the environment. Some traditional technologies, such as adsorption and microwave catalysis, are applied to treat the wastewater before discharging [1–3]. Some kinds of organic materials are even harmful to microorganisms, so that the well-applied bio-chemical technique cannot be used to such kinds of wastewater. Besides, advanced oxidation methods such as photocatalytic oxidation technique has been studied for decades to deal with most kinds of hazardous organic pollutants [4–6]. Interestingly, researchers have reported the fully decomposition of various kinds of organic pollutants, for example, dyes and antibiotics [7,8].

Photocatalyst is the most important factor and the research focus in this field, for example, titania has be regarded as the well-applied photocatalytic material [9,10]. Moreover, the development of novel and powerful photocatalytic material is always interesting. Pyrochloro or perovskite structured titanates have been proven to be potential photocatalytic material [11–15]. The properties of titanates may be different with the variation of cationic element in the materials [16–19]. Modification of titanate is also necessary to improve its activity. For example, bisphenol A in water could be decomposed on nitrogen-doped perovskite-type $La_2Ti_2O_7$ [20]. Dye decolorization was enhanced after loading $La_2Ti_2O_7$ on HZSM-5 zeolite [21].

Azophloxine is an azo dye that can be removed from the wastewater by adsorption or by the overall mineralization of the organic compound [22,23]. Adsorption of organic substance on photocatalytic material is the primary step, because photogenerated oxidative reagents such as hydroxyl radicals may migrate to the surface of photocatalytic material and react with the adsorbed organic substances to complete the degradation step.

* Corresponding author.

High temperature thermal treatment cannot be avoided to synthesize titanate because crystallization of titanate usually occurs at high temperature. The photocatalytic activity of titanate is constrained by particles aggregation in the material, and the obtained material does not have porous structure. In order to promote porosity of titanate, a successful way is the use of pore forming reagent. The increment in surface area of TiO_2 nanowires is responsible for the enhancement in atrazine degradation efficiency [24]. Polyethylene glycol could modify the porosity of TiO_2–$InVO_4$ nanoparticles for effective photocatalytic degradation of methylene blue [25]. It is an interesting attempt to improve the activity of titanate by forming pores in the material.

We reported the role of PEG2000 in sol–gel preparation of porous $La_2Ti_2O_7$ [26]. In this work, the materials were used for photocatalytic degradation of azophloxine, an azo dye. The focus of this work is to examine photocatalytic degradation of azophloxine. The azophloxine solution during photocatalytic degradation process was studied using Fourier transform infrared spectroscopy (FT-IR), UV-visible (UV-Vis) spectrometry, total organic carbon (TOC) analysis, and ion chromatography.

2. Experimental methods

2.1. Photocatalytic activity measurement

Photocatalytic activity of the obtained lanthanum titanate was determined in a lab-scale reactor that was made of a 20 W UV lamp and a 100 mL quartz beaker. The initial concentration of azophloxine solution was 40 mg L^{-1}. Fifty milliliters of azophloxine solution and 30 mg lanthanum titanate sample were stirred in the dark for 30 min to reach adsorption–desorption equilibrium. Photocatalytic degradation of azophloxine was also analyzed after turning on the UV lamp. The concentration of the azophloxine solution was measured by a 721E spectrophotometer at the maximum absorption wavelength of 506 nm. The degradation efficiency was calculated using $[(C_0 - C)/C_0] \times 100\%$. Here, C_0 is the initial azophloxine concentration and C is the azophloxine concentration in the solution.

2.2. Determination of azophloxine solution

The mixture of azophloxine solution and photocatalyst was centrifuged at 11,000 rpm for 10 min, and the was filtrated through a 0.45 μm Millipore filter before the determinations of FT-IR, UV-Vis spectrometry, TOC, and ion chromatography. Fifteen milliliters of azophloxine solution was dried at 40°C. The obtained solid was dissolved in 1 mL methane, and the solution was mixed with 100 mg KBr. The mixture was dried at 30°C before taking infrared spectrum on a Frontier FT-IR/FIR spectrometer. The UV-Vis spectra of azophloxine solution were recorded by a LAMBDA 35 UV-Vis spectrometer. TOC of the azophloxine solution was measured by an multi N/C 3,100 TOC/TN analyzer. The combustion furnace temperature was 850°C. The concentrations of Na^+, NH_4^+, NO_2^-, NO_3^-, and SO_4^{2-} ions were determined by an ICS1100 ion chromatograph, which was equipped with an AERS 500 (4 mm) anion suppressor, a CERS 500 (4 mm) cation suppressor, an IonPac AS11-HC (4 × 250 mm) anion analytical column and a CS12A (4 mm) cation analytical column.

3. Results and discussion

3.1. Photocatalytic degradation of azophloxine

Porous perovskite $La_2Ti_2O_7$ photocatalyst was synthesized via a sol–gel route in our previous work [26]. The materials were characterized using X-ray powder diffraction, scanning electron microscopy (SEM), UV-Vis spectrometry, surface area and pore analysis, and X-ray photoelectron spectroscopy. We will not repeat the detailed characterization results in the current work, but the brief experimental results need to be summarized. Restrained crystal aggregation and porous structure can be observed in the SEM and TEM images of the porous samples. The addition of PEG2000 can apparently influence porosity of the materials. The $La_2Ti_2O_7$ sample prepared using 3 g of PEG2000 has both the maximum BET surface area and pore volume.

Fig. 1 shows photocatalytic degradation of azophloxine on the $La_2Ti_2O_7$ materials. In prior to photocatalytic oxidation, the dye solution and $La_2Ti_2O_7$ powders were stirred in the dark to ensure adsorption–desorption equilibrium. The number of the adsorbed azophloxine molecules on the samples does not change with the variation of PEG2000 amount. The percentage of azophloxine molecules removed by adsorption is not more than 2.5% on all the samples. The azophloxine molecules and the $La_2Ti_2O_7$ powders do not have enough affinity.

Photocatalytic degradation of azophloxine can be improved by the addition of PEG2000. The porous $La_2Ti_2O_7$ sample obtained with 3 g of PEG2000 has the maximum photocatalytic activity. The decline of photocatalytic activity can be observed when 5 g of PEG2000 is used. Photocatalytic activity of the porous $La_2Ti_2O_7$ samples is in accordance to the variation of BET surface area. 98.5% of the azophloxine molecules are degraded after 180 min of irradiation on the $La_2Ti_2O_7$ sample obtained with 3 g of PEG2000, while much longer time is needed for the $La_2Ti_2O_7$ sample prepared without PEG2000.

The porous $La_2Ti_2O_7$ sample obtained with 3 g of PEG2000 was reused to examine the reusability. The azophloxine solution was restored to the initial concentration after 180 min of irradiation in each cycle. Photocatalytic degradation efficiency is 98.5% in the first cycle, and the efficiency is 91.9% in the fifth cycle. The slight decline of degradation efficiency can be attributed to the loss of fine $La_2Ti_2O_7$ powders when taking solution sample for examination.

3.2. Determination of azophloxine solution

The UV-Vis spectra of azophloxine solution during photocatalytic degradation on the porous $La_2Ti_2O_7$ samples are presented in Fig. 2. The characteristic group in azophloxine molecule is the azo conjugated system. This is the major chromophore group of the azo dye that has strong absorption at 506 nm. The intrinsic absorption of benzene ring and naphthalene ring is at 235 nm, while the absorption at 320 nm is due to the interplay of benzene ring and naphthalene ring with the chromophore group. The weak absorption peak at 249 nm is related to n–π conjugated absorption of secondary amide.

There are still strong absorptions in the whole spectra for the nonporous sample after 240 min of irradiation, while the

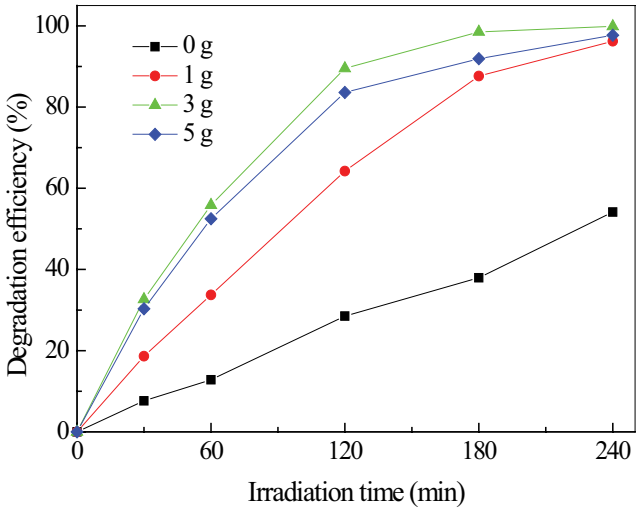

Fig. 1. Photocatalytic degradation of azophloxine on the $La_2Ti_2O_7$ materials with prolonged irradiation time.

porous sample obtained using 3 g PEG2000 can lead to nearly overall degradation of azophloxine molecule after only 180 min of reaction. The organic groups in azophloxine can be degraded during photocatalytic oxidation process, which is proven by the reduced absorption intensity in the UV-Vis spectra. Apparently, the dropping off rate of the absorption intensity can be used to identify photocatalytic activity of the $La_2Ti_2O_7$ samples. The $La_2Ti_2O_7$ sample obtained using 3 g of PEG2000 can lead to the fastest reducing rate of all the absorption intensities in both the visible and ultraviolet regions.

Fig. 3 shows the UV-Vis spectra of azophloxine solution with respect to PEG2000 amount after 60 and 180 min of photocatalytic degradation. The photocatalytic activity sequence of the materials can be identified in the spectra. The $La_2Ti_2O_7$ sample obtained without PEG2000 has the lowest activity, while the activity of the porous samples also differs from each other in dependence of PEG2000 amount. All the major absorption peaks in the whole spectrum are reduced during photocatalytic degradation of azophloxine. As shown in Fig. 3b, the $La_2Ti_2O_7$ samples obtained using more than 2 g

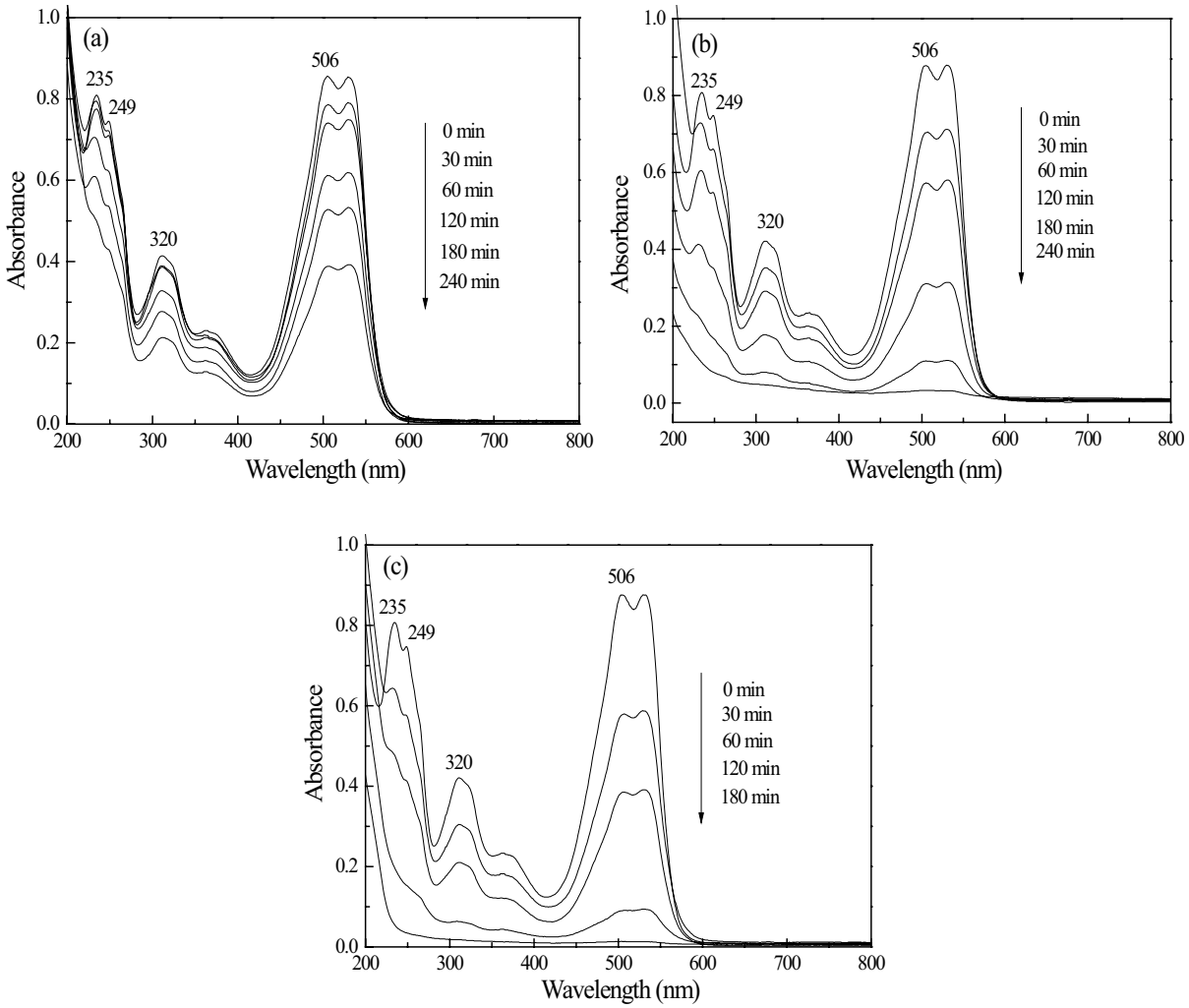

Fig. 2. UV-Vis spectra of azophloxine solution during photocatalytic degradation on the porous $La_2Ti_2O_7$ samples obtained (a) without PEG2000, (b) using 1 g PEG2000, and (c) using 3 g PEG2000.

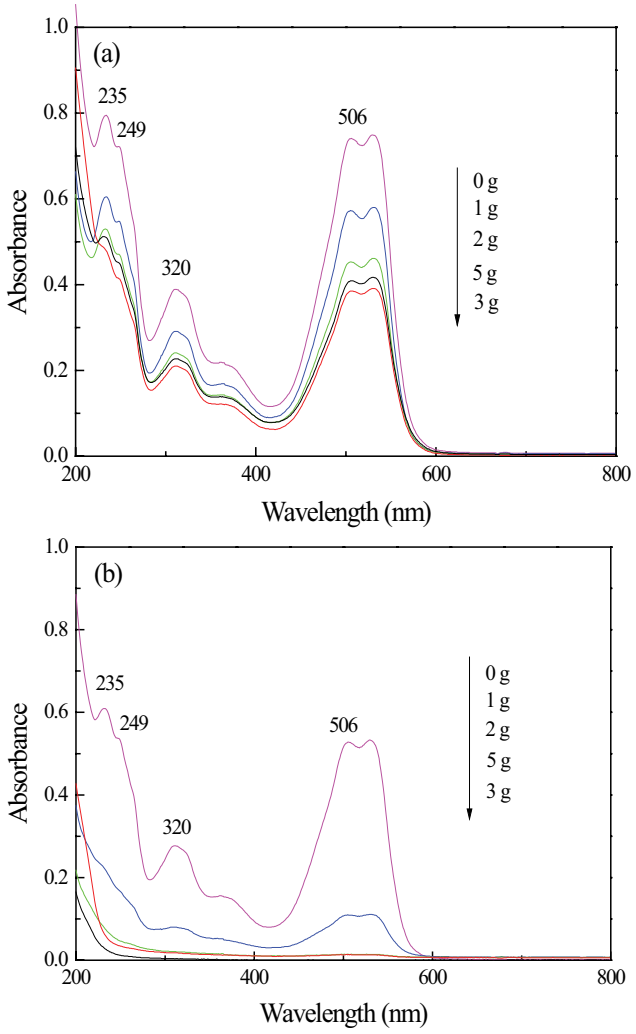

Fig. 3. UV-Vis spectra of azophloxine solution with respect to PEG2000 amount after (a) 60 min and (b) 180 min of photocatalytic degradation.

of PEG2000 can degrade nearly all of the organic groups in azophloxine molecules after 180 min of irradiation.

Fig. 4 presents the FT-IR spectra of azophloxine solution during photocatalytic degradation on the porous $La_2Ti_2O_7$ samples. As a complex azo dye, the azophloxine molecule has characteristic infrared absorption in the wavenumber range between 500 and 4,000 cm^{-1}. The absorption peak at 634 cm^{-1} is related to in-plane bending vibration of naphthalene ring, the peak at 988 cm^{-1} is due to bending vibration of C–H bond on both benzene ring and naphthalene ring, and the skeleton stretching vibrations of benzene ring and naphthalene ring are observed at 1,456; 1,496; and 1,564 cm^{-1} [27]. Carbonyl group has an absorption at 1,614 cm^{-1}, and the vibration of C–O bond in organic acid or ester has an absorption at 1,108 cm^{-1} [28]. The stretching vibration of C–N bond can be observed at 1,400 cm^{-1}, while the absorptions at 1,050 and 1,214 cm^{-1} are attributed to R–SO_3^- [29]. The stretching vibrations of methyl and methylene groups have absorptions at 2,928 and 2,856 cm^{-1}. The out-of-plane bending vibration of N–H bond in the amide group of azophloxine has absorption at 756 cm^{-1}, while the broad absorption centered at 3,445 cm^{-1} is due to the vibrations of N–H and O–H bonds [30]. The sharp absorption peak at 1,382 cm^{-1} is attributed to bending vibration of –OH in carboxylic acids.

The variation of FT-IR spectra of azophloxine solution during degradation can be clearly identified in Fig. 4c. Degradation of azophloxine results in decomposition of the characteristic groups in the molecule, and therefore oxidation products might be formed during photocatalytic oxidation process. The absorption of in-plane bending vibration of naphthalene ring undergoes a blue shift during degradation, indicating the breakup of naphthalene ring. The cyclic olefinic bond is weakened at the decomposed naphthalene ring. The same phenomenon can also be observed for skeleton stretching vibrations of benzene ring and naphthalene ring at 1,456; 1,496; and 1,564 cm^{-1}, since these absorptions disappear after 120 min of irradiation. The bending vibration of C–H bond at 988 cm^{-1} is reduced with extended reaction time.

The R–SO_3^- group in azophloxine molecule is broken up to release SO_4^{2-} ion, accompanied by the decreased absorption at 1,050 and 1,214 cm^{-1}. Benzene rings are totally decomposed and the residues are small organic substances containing carbonyl group or carboxyl group, showing by the slightly raised absorption at 1,108 cm^{-1}. The stretching vibrations of methyl and methylene still have weak absorptions at 2,928 and 2,856 cm^{-1} after 240 min of reaction, showing the existence of organic substances in the solution. Meanwhile, the change of C=O absorption at 1,614 cm^{-1} is quite small with the variation of reaction time, since the carbonyl group is hardly decomposed during photocatalytic oxidation.

Fig. 5 shows the FT-IR spectra of azophloxine solution with respect to PEG2000 amount after 60 and 180 min of photocatalytic degradation. The effects of PEG2000 addition on degradation of the groups in azophloxine molecule can be clarified. The spectra in Fig. 5a cannot show apparent difference with the variation of PEG2000 amount since the reaction time is only 60 min. Whereas, many differences can be observed after 180 min of reaction, as shown in Fig. 5b. Degradation of azophloxine can be accomplished much quicker if the material has better activity. This can be proven by the enhanced degradation rates of the groups in azophloxine molecule and by the formation of intermediates and final oxidation products.

When the porous $La_2Ti_2O_7$ samples are used as photocatalyst, the degradation of benzene ring, naphthalene ring, C–N bond, and R–SO_3^- can be ensured because the corresponding absorptions at 1,456; 1,496; 1,564; 1,400; 1,050; and 1,214 cm^{-1} disappear after 180 min of irradiation. The oxidation products of benzene rings and naphthalene rings are small organic substances containing carbonyl group or carboxyl group, whose strong absorption can be seen at 1,108 cm^{-1}. The formation of small organic acids in the solution also results in the sharp absorption peak at 1,382 cm^{-1}, attributing to bending vibration of –OH in carboxylic acids.

Fig. 6 shows TOC removal in azophloxine solution during photocatalytic degradation. As an advanced oxidation technique, photocatalytic oxidation of organic substance can lead to partial or complete mineralization of many kinds of hazardous pollutants. The mineralization can be measured by

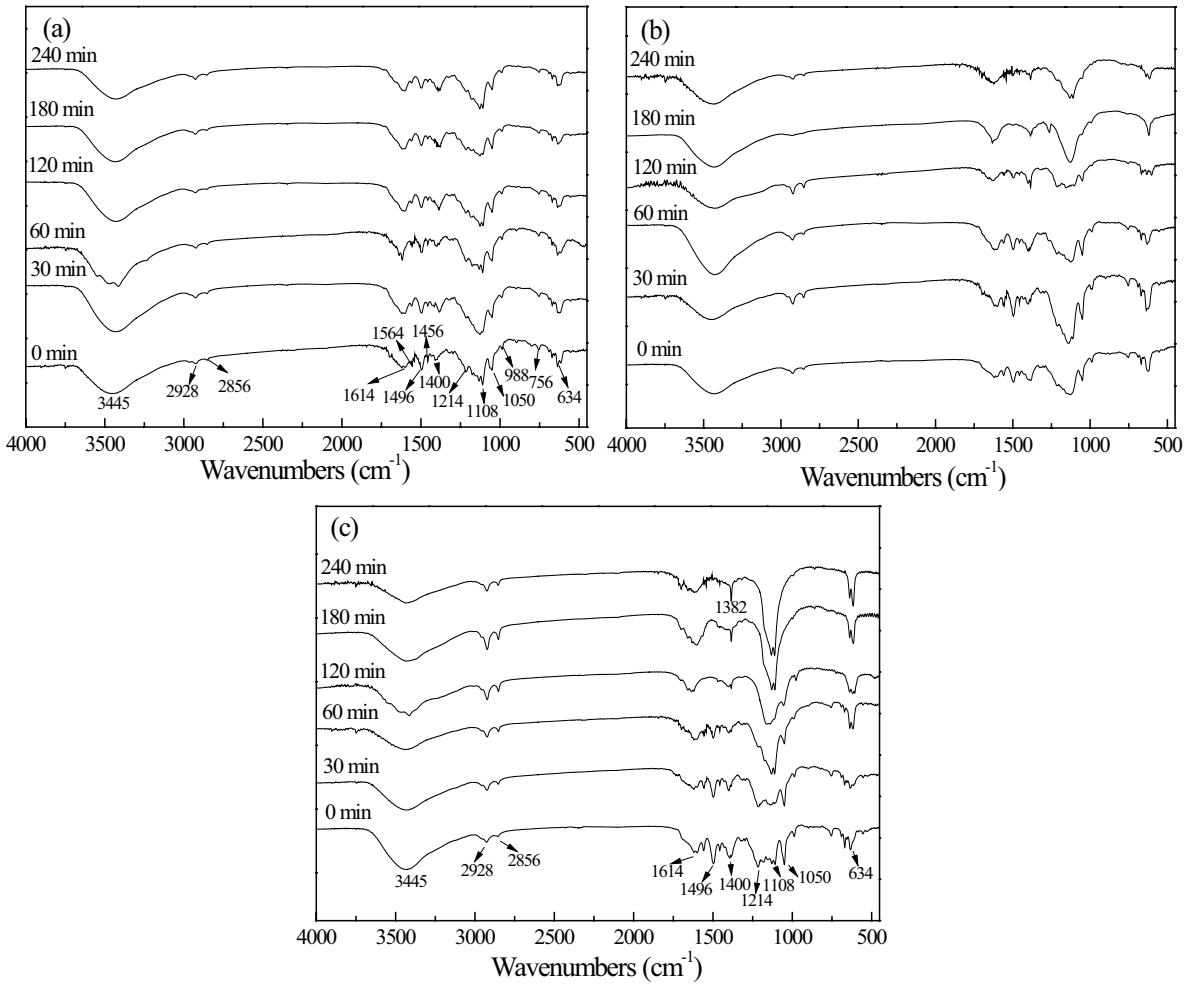

Fig. 4. FT-IR spectra of azophloxine solution during photocatalytic degradation on the porous $La_2Ti_2O_7$ samples obtained (a) without PEG2000, (b) using 1 g PEG2000, and (c) using 3 g PEG2000.

TOC removal efficiency during photocatalytic degradation process. Although all the $La_2Ti_2O_7$ samples have the ability on oxidizing azophloxine, mineralization efficiency depends on the activity of the materials.

As stated before, azophloxine can be fully decolorized after 180 min of photocatalytic degradation, and at this time, the major chromophore groups in both visible and ultraviolet regions are decomposed into small fractions. However, it does not mean that all the organic substances have been converted into CO_2 and H_2O. The $La_2Ti_2O_7$ sample obtained using 3 g PEG2000 can decolorize all the azophloxine molecules in 180 min. Meanwhile, TOC removal efficiency is only 67.5% after 240 min of irradiation. As shown in Fig. 6, TOC values in the solution are nearly unchanged in the first 30 min during photocatalytic degradation. The large azophloxine molecule has to be broken up into small intermediates at the beginning, and the intermediates can be subsequently degraded. Oxidation of the organic substances into CO_2 and H_2O in the solution may take longer time.

Fig. 7 shows ion concentrations in azophloxine solution during photocatalytic degradation as a function of PEG2000 amount. The changes of Na^+, NH_4^+, NO_2^-, NO_3^-, and SO_4^{2-} concentrations in the azophloxine solution during degradation can give information on degradation products. As shown in Fig. 7a, the Na^+ ion concentration of 3.6 mg L^{-1} is nearly unchanged during the whole period, because Na^+ ions dissociate into the solution as free ions right after dissolving of azophloxine. The –N=N– azo group and R_2–N–H group are broken up from azophloxine molecule, and the nitrogen-containing intermediates can subsequently be oxidized to produce NH_4^+, NO_2^-, and NO_3^- ions. As shown in Fig. 7b, the NH_4^+ concentration constantly increases in all the solutions during degradation process, and more NH_4^+ ions are produced in the solution containing stronger photocatalyst. The NH_4^+ concentration in the initial azophloxine solution is small, so that most of the NH_4^+ ions are the degradation product of –N=N– azo group and R_2–N–H group in azophloxine.

Nitrogen in azophloxine can be oxidized to produce N_2, NO_2^-, and NO_3^-. The concentrations of NO_2^- and NO_3^- ions in the solution also vary during degradation process, as shown in Figs. 7c and d. The initial azophloxine solution has the maximum concentration of NO_2^- ion, and the concentration of NO_2^- ion decreases constantly under irradiation. Apparently,

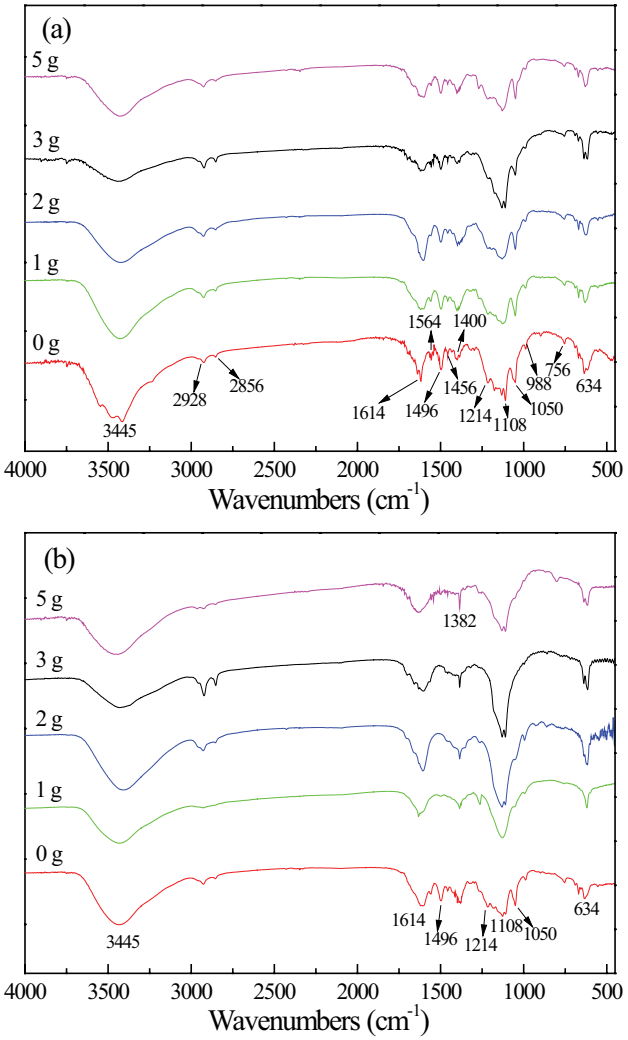

Fig. 5. FT-IR spectra of azophloxine solution with respect to PEG2000 amount after (a) 60 min and (b) 180 min of photocatalytic reaction.

the NO_2^- ions come from the impurity in the azophloxine dye, and can hardly be the oxidation product of –N=N– azo group and R_2–N–H group in azophloxine. The NO_2^- ions are unstable during photocatalytic process, and are transformed into other nitrogen containing species. NO_3^- ions are also produced during photocatalytic reaction of azophloxine, and the number of NO_3^- ions depends on the activity of the materials. The original NO_3^- ion concentration in the azophloxine solution is quite small, which is as similar as NH_4^+ ion concentration.

Sulfur in azophloxine is oxidized to SO_4^{2-} ion, as shown in Fig. 7e. There is no SO_4^{2-} ion in the original solution of azophloxine, and all the SO_4^{2-} ions are the oxidation product of sulfonic acid group in azophloxine molecule. The concentration of SO_4^{2-} ion constantly increases during photocatalytic oxidation, according to the activity of the $La_2Ti_2O_7$ samples. With the existence of the $La_2Ti_2O_7$ sample obtained using 3 g of PEG2000, the SO_4^{2-} ion concentration in the solution is 14.0 mg L^{-1} after 240 min of irradiation.

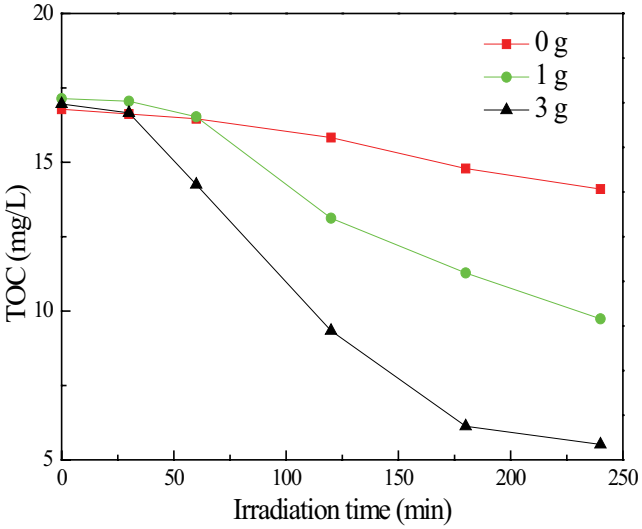

Fig. 6. Total organic carbon removal in azophloxine solution during photocatalytic degradation.

Since the theoretical concentration of SO_4^{2-} ion in 40 mg L^{-1} azophloxine solution is 15.1 mg L^{-1}, nearly all of the sulfonic acid groups in azophloxine molecule are degraded into SO_4^{2-} ions. This is in accordance to the results obtained in FT-IR spectra.

Fig. 8 shows ionic nitrogen concentration in azophloxine solution during degradation. Organic nitrogen in azophloxine molecule can be degraded into NH_4^+, NO_2^-, and NO_3^- ions. The final degradation products of nitrogen are NH_4^+ and NO_3^- ions, and NO_2^- ion is not stable during photocatalytic oxidation. The total ionic nitrogen concentration in the solution increases with rising reaction time, depending on the activity of the materials. In presence of the $La_2Ti_2O_7$ sample obtained using 3 g of PEG2000, the ionic nitrogen concentration is 0.688 mg L^{-1} after 240 min photocatalytic degradation. The ionic nitrogen is much smaller than the theoretical nitrogen content of 3.32 mg L^{-1} in the original azophloxine solution. As mentioned before, TOC removal efficiency is only 67.5% after 240 min of irradiation. Nitrogen can also be reduced to produce molecular nitrogen, and gaseous N_2 can be released from the solution.

4. Conclusions

Photocatalytic degradation of azophloxine can be improved by the addition of PEG2000 in sol–gel synthesizing of porous $La_2Ti_2O_7$. When PEG2000 amount is increased from 0 to 3 g, photocatalytic degradation efficiency in 60 min increases from 12.8% to 55.9%. The reduced absorption intensity in both UV-Vis and FT-IR spectra of azophloxine solution demonstrates photocatalytic degradation of azophloxine on the $La_2Ti_2O_7$ samples. Mineralization of the organic substances is slower than decoloration of the dye. Degradation of azophloxine can be accomplished much quicker on the material possessing higher activity, which can be proven by the enhanced degradation rates of the organic groups in azophloxine molecule.

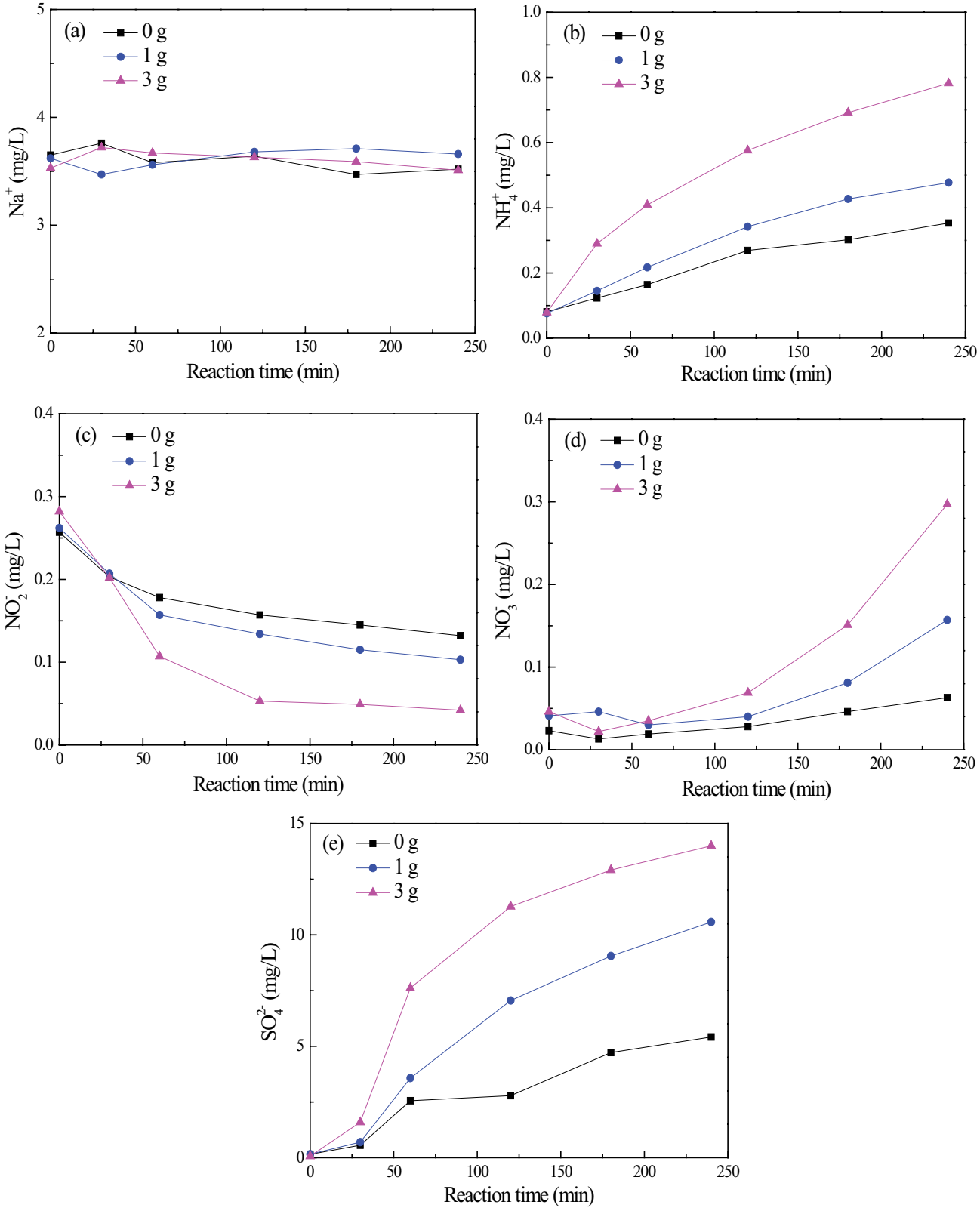

Fig. 7. Ion concentrations in azophloxine solution during photocatalytic degradation as a function of PEG2000 amount. (a) Na^+, (b) NH_4^+, (c) NO_2^-, (d) NO_3^-, and (e) SO_4^{2-}.

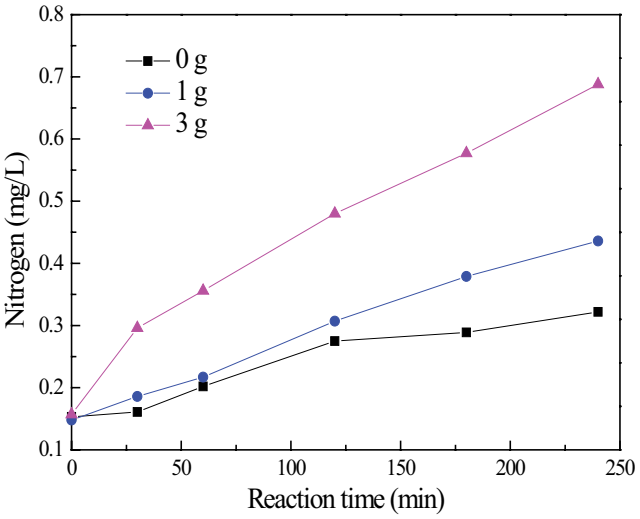

Fig. 8. Ionic nitrogen concentration in azophloxine solution during degradation.

Acknowledgments

This work was supported by Scientific Research Fund of Liaoning Provincial Education Department (No. LG201923).

References

[1] Y.Q. Yang, D.W. Wen, Q. Ding, Y. Wang, N. Liu, Y.X. Zhao, X.D. Zhang, Adsorption behavior of perchlorate removal from aqueous solution using MgAlCe hydrotalcite-like compounds, Desal. Water Treat., 88 (2017) 257–267.
[2] Y.Q. Yang, Z.H. Zheng, D.F. Zhang, X.D. Zhang, Response surface methodology directed adsorption of chlorate and chlorite onto MIEX resin and study of chemical properties, Environ. Sci. Water Res. Technol., (2020), doi: 10.1039/C9EW01003C.
[3] Y. Wang, L. Yu, R. Wang, Y. Wang, X.D. Zhang, Microwave catalytic activities of supported perovskite catalysts MO_x/$LaCo_{0.5}Cu_{0.5}O_3$@CM (M = Mg, Al) for salicylic acid degradation, J. Colloid Interface Sci., 564 (2020) 392–405.
[4] M.R. Hoffmann, S.T. Martin, W. Choi, W. Bahnemann, Environmental applications of semiconductor photocatalysis, Chem. Rev., 95 (1995) 69–96.
[5] A. Fujishima, T.N. Rao, D.A. Tryk, Titanium dioxide photocatalysis, J. Photochem. Photobiol., C, 1 (2000) 1–21.
[6] S. Zinatloo-Ajabshir, Z. Salehi, M. Salavati-Niasari, Green synthesis and characterization of $Dy_2Ce_2O_7$ ceramic nanostructures with good photocatalytic properties under visible light for removal of organic dyes in water, J. Cleaner Prod., 192 (2018) 678–687.
[7] Z. Li, M. Qi, C. Tu, W. Wang, J. Chen, A.J. Wang, Highly efficient removal of chlorotetracycline from aqueous solution using graphene oxide/TiO_2 composite: properties and mechanism, Appl. Surf. Sci., 425 (2017) 765–775.
[8] G. Sharma, S. Bhogal, M. Naushad, A. Kumar, F.J. Stadler, Microwave assisted fabrication of La/Cu/Zr/carbon dots trimetallic nanocomposites with their adsorptional vs photocatalytic efficiency for remediation of persistent organic pollutants, J. Photochem. Photobiol., A, 347 (2017) 235–243.
[9] K. Nakata, A. Fujishima, TiO_2 photocatalysis: design and applications, J. Photochem. Photobiol., C, 13 (2012) 169–189.
[10] V. Likodimos, Photonic crystal-assisted visible light activated TiO_2 photocatalysis, Appl. Catal., B, 230 (2018) 269–303.
[11] F. Li, K. Yu, L. Lou, Z. Su, S. Liu, Theoretical and experimental study of La/Ni co-doped $SrTiO_3$ photocatalyst, Mater. Sci. Eng., B, 172 (2010) 136–141.
[12] J. Chen, S. Liu, L. Zhang, N. Chen, New SnS_2/$La_2Ti_2O_7$ heterojunction photocatalyst with enhanced visible-light activity, Mater. Lett., 150 (2015) 44–47.
[13] W. Zhang, Y. Liu, C. Li, Photocatalytic degradation of ofloxacin on $Gd_2Ti_2O_7$ supported on quartz spheres, J. Phys. Chem. Solids, 118 (2018) 144–149.
[14] Z. Chen, H. Jiang, W. Jin, C. Shi, Enhanced photocatalytic performance over $Bi_4Ti_3O_{12}$ nanosheets with controllable size and exposed {001} facets for Rhodamine B degradation, Appl. Catal., B, 180 (2016) 698–706.
[15] W.J. Zhang, Y.J. Tao, C.G. Li, Effects of PEG4000 template on sol–gel synthesis of porous cerium titanate photocatalyst, Solid State Sci., 78 (2018) 16–21.
[16] W.J. Zhang, J. Yang, C.G. Li. Role of thermal treatment on sol–gel preparation of porous cerium titanate: characterization and photocatalytic degradation of ofloxacin, Mater. Sci. Semicond. Process., 85 (2018) 33–39.
[17] Y.A. Zulueta, M.T. Nguyen, Multisite occupation of divalent dopants in barium and strontium titanates, J. Phys. Chem. Solids, 121 (2018) 151–156.
[18] B. Kiss, T.D. Manning, D. Hesp, C. Didier, M.J. Rosseinsky, Nano-structured rhodium doped $SrTiO_3$–visible light activated photocatalyst for water decontamination. Appl. Catal., B, 206 (2017) 547–555.
[19] W.J. Zhang, Y.J. Tao, C.G. Li, Sol–gel synthesis and characterization of $Gd_2Ti_2O_7$/SiO_2 photocatalyst for ofloxacin decomposition, Mater. Res. Bull., 105 (2018) 55–62.
[20] Z.L. Hua, X.Y. Zhang, X. Bai, L.L. Lv, Z.F. Ye, X. Huang, Nitrogen-doped perovskite-type $La_2Ti_2O_7$ decorated on graphene composites exhibiting efficient photocatalytic activity toward bisphenol A in water, J. Colloid Interface Sci., 450 (2015) 45–53.
[21] W.J. Zhang, Z. Ma, L. Du, L.L. Yang, X.J. Chen, H.B. He, Effects of calcination temperature on characterization and photocatalytic activity of $La_2Ti_2O_7$ supported on HZSM-5 zeolite, J. Alloys Compd., 695 (2017) 3541–3546.
[22] E. Bicer, C. Arat, A voltammetric study on the aqueous electrochemistry of Acid Red 1 (Azophloxine), Croat. Chem. Acta, 82 (2009) 583–592.
[23] A. Mehrizad, M.A. Behnajady, P. Gharbani, S. Sabbagh, Sonocatalytic degradation of Acid Red 1 by sonochemically synthesized zinc sulfide-titanium dioxide nanotubes: optimization, kinetics and thermodynamics studies, J. Cleaner Prod., 215 (2019) 1341–1350.
[24] Y. Zhang, C. Han, G. Zhang, D. Dionysiou, M. Nadagoudaf, PEG-assisted synthesis of crystal TiO_2 nanowires with high specific surface area for enhanced photocatalytic degradation of atrazine, Chem. Eng. J., 268 (2015) 170–179.
[25] H. Chang, E. Jo, H. Jang, T. Kim, Synthesis of PEG-modified TiO_2-$InVO_4$ nanoparticles via combustion method and photocatalytic degradation of methylene blue, Mater. Lett., 92 (2013) 202–205.
[26] H. Wang, Y. Zhang, Z. Ma, W. Zhang, Role of PEG2000 on sol–gel preparation of porous $La_2Ti_2O_7$ for enhanced photocatalytic activity on ofloxacin degradation, Mater. Sci. Semicond. Process., 91 (2019) 151–158.
[27] X. Gao, L. Zhang, M. Sun, Y. Xiao, J. Su, Fast zero-order hydrocracking reaction of X-3B over crystal Al–Fe alloys: effect of electrochemical corrosion behaviors, Mater. Des., 109 (2016) 570–579.
[28] C. Zhang, S. Yang, H. Chen, H. He, C. Sun, Adsorption behavior and mechanism of reactive brilliant red X-3B in aqueous solution over three kinds of hydrotalcite-like LDHs, Appl. Surf. Sci., 301 (2014) 329–337.
[29] X.L. Li, X.M. Xie, H.H. Luo, L. Li, Z. Li, Z.Y. Xue, W. Li, Adsorption of reactive yellow X-RG and reactive brilliant red X-3B onto cucurbit [8] uril and cucurbit [6] uril: effect factors, adsorption behavior and mechanism study, J. Colloid Interface Sci., 498 (2017) 31–46.
[30] B.K. Shanmugama, S.N. Easwarana, R. Lakra, P.R. Deepa, S. Mahadevan, Metabolic pathway and role of individual species in the bacterial consortium for biodegradation of azo dye: a biocalorimetric investigation, Chemosphere, 188 (2017) 81–89.